



ALMA MATER STUDIORUM  
UNIVERSITÀ DI BOLOGNA

ARCHIVIO ISTITUZIONALE  
DELLA RICERCA

## Alma Mater Studiorum Università di Bologna Archivio istituzionale della ricerca

Testing the impact of discoplasty on the biomechanics of the intervertebral disc with simulated degeneration:  
An in vitro study

This is the final peer-reviewed author's accepted manuscript (postprint) of the following publication:

*Published Version:*

Testing the impact of discoplasty on the biomechanics of the intervertebral disc with simulated degeneration: An in vitro study / Techens C.; Palanca M.; Eltes P.E.; Lazary A.; Cristofolini L.. - In: MEDICAL ENGINEERING & PHYSICS. - ISSN 1350-4533. - STAMPA. - 84:(2020), pp. 51-59. [10.1016/j.medengphy.2020.07.024]

*Availability:*

This version is available at: <https://hdl.handle.net/11585/808871> since: 2021-02-27

*Published:*

DOI: <http://doi.org/10.1016/j.medengphy.2020.07.024>

*Terms of use:*

Some rights reserved. The terms and conditions for the reuse of this version of the manuscript are specified in the publishing policy. For all terms of use and more information see the publisher's website.

This item was downloaded from IRIS Università di Bologna (<https://cris.unibo.it/>).  
When citing, please refer to the published version.

(Article begins on next page)

This is the final peer-reviewed accepted manuscript of:

**Med Eng Phys. 2020 Oct;84:51-59. doi:  
10.1016/j.medengphy.2020.07.024. Epub 2020 Jul 30.**

**Testing the impact of discoplasty on the biomechanics of the  
intervertebral disc with simulated degeneration: An in vitro study**

Chloé Techens, Marco Palanca, Peter Endre Éltés, Áron Lazáry, Luca  
Cristofolini

PMID: 32977922 DOI: 10.1016/j.medengphy.2020.07.024

The final published version is available online at:

<https://doi.org/10.1016/j.medengphy.2020.07.024>

Rights / License:

The terms and conditions for the reuse of this version of the manuscript are specified in the publishing policy. For all terms of use and more information see the publisher's website.

**Testing the impact of discoplasty on the biomechanics of the  
intervertebral disc with simulated degeneration:  
an *in vitro* porcine study**

Chloé Techens, MEng <sup>1</sup>, Marco Palanca, Ph.D. <sup>1</sup>, Peter Endre Eltes MD <sup>2</sup>,  
Aron Lazary PhD <sup>2</sup>, Luca Cristofolini, Ph.D. <sup>1</sup>

<sup>1</sup> Department of Industrial Engineering, School of Engineering and Architecture, Alma  
Mater Studiorum - Università di Bologna, Bologna, Italy

<sup>2</sup> R&D Department of National Center for Spinal Disorders, Budapest, Hungary

***Submitted to:* Medical Engineering & Physics, special issue “Biomechanics for in  
silico clinical trials: thematic symposium of the IX Meeting of the Italian Chapter  
of the European Society of Biomechanics”**

***Original submission:*** 4<sup>th</sup> March 2020

***Revised version:*** 18<sup>th</sup> July 2020

***Statistics:***

|                          |              |
|--------------------------|--------------|
| Word count (manuscript): | @ 4890 words |
| Word count (abstract):   | @ 238 words  |
| Figures:                 | @ 9          |
| Tables:                  | @ 2          |
| References:              | @ 43         |

***Corresponding author:***

Luca Cristofolini  
Department of Industrial Engineering  
School of Engineering and Architecture  
University of Bologna  
Viale Risorgimento, 2  
40136 Bologna, Italy  
e-mail: [luca.cristofolini@unibo.it](mailto:luca.cristofolini@unibo.it)

1 **ABSTRACT**

2 Percutaneous Cement Discoplasty has recently been developed to relieve pain in highly  
3 degenerated intervertebral discs presenting a vacuum phenomenon in patients that  
4 cannot undergo major surgery. Little is currently known about the biomechanical effects  
5 of discoplasty. This study aimed at investigating the feasibility of modelling empty discs  
6 and subsequent discoplasty surgery and measuring their impact over the specimen  
7 geometry and mechanical behavior. Ten porcine lumbar spine segments were tested in  
8 flexion, extension, and lateral bending under 5.4 Nm (with a 200 N compressive force  
9 and a 27 mm offset). Tests were performed in three conditions for each specimen: with  
10 intact disc, after nucleotomy and after discoplasty. A 3D Digital Image Correlation  
11 (DIC) system was used to measure the surface displacements and strains. The posterior  
12 disc height, range of motion (ROM), and stiffness were measured at the peak load. CT  
13 scans were performed to confirm that the cement distribution was acceptable.  
14 Discoplasty recovered the height loss caused by nucleotomy ( $p=0.04$ ) with respect to  
15 the intact condition, but it did not impact significantly either the ROM or the stiffness.  
16 The strains over the disc surface increased after nucleotomy, while discoplasty  
17 concentrated the strains on the endplates. In conclusion, this preliminary study has  
18 shown that discoplasty recovered the intervertebral posterior height, opening the  
19 neuroforamen as clinically observed, but it did not influence the spine mobility or  
20 stiffness. This study confirms that this *in vitro* approach can be used to investigate  
21 discoplasty.

22 **Keywords:**

23 Percutaneous Cement Discoplasty, Spine, Biomechanical testing, Strain

## 24 1. INTRODUCTION

25 Intervertebral Disc (IVD) degeneration is one of the main causes of low back pain, a  
26 large socio-economic burden for society, affecting between 60% and 70% of the  
27 population in industrialized countries at least once during their lifetimes [1]. Interbody  
28 fusion with the insertion of an intervertebral spacer after performing disc fenestration is  
29 the most common surgical treatment and has been widely studied in the literature [2]–  
30 [10]. It requires an invasive surgery which lasts for hours and is often associated with  
31 significant blood loss, long recovery, and general anaesthesia which is not suitable for  
32 elderly patients or those with significant comorbidities. Since this disease appears with  
33 age, finding minimally invasive treatments is crucial to treat the most complex cases.  
34 Percutaneous Cement Discoplasty (PCD), a surgical technique that minimizes the  
35 surgical morbidity and complication risks, is applied when a vacuum phenomenon is  
36 observed inside the IVD, resulting in the collapse of the adjacent vertebra and in nerve  
37 root compression. It consists of injecting an polymethylmethacrylate cement (PMMA)  
38 to “create individually shaped “in-site” intervertebral spacers” in order to recover the  
39 disc height and decompress the spinal canal [11]. One advantage of using PMMA to  
40 stabilize the spine is that “the load-bearing surface of the implant is fully adapted to the  
41 shape of the endplates”.

42

43 PCD is a newly developed technique, the authors found very little literature on the  
44 subject. Varga *et al* presented in 2015 the technique and their clinical study on 47  
45 patients showed significant improvement in their quality of life, correlating with a pain  
46 factor decrease at 6 month follow-up [11]. Another study reported the surgery of a  
47 patient treated with PCD [12]. Discoplasty was shown to positively affect the spinal  
48 alignment and neuro-foraminal height in 27 patients [13].

49 While the impact of PCD on spine has been clinically assessed by comparing pre-  
50 operative/post-operative scores, no indication about spine kinetics and kinematics has  
51 been found by the authors. Some studies investigated similar techniques on animals,  
52 performing *in vitro* testing of spines in intact condition (with a full IVD), after removal  
53 of the Nucleus Pulposus (NP), and/or after a stabilization surgery. Refilling of the disc  
54 with soft materials [14] to recover intact spine mechanics was also investigated,

55 however it differs from discoplasty which uses acrylic cement. Only Moissonier *et al*  
56 and Wilke *et al* mimicked the PCD technique, implanting a spacer within the empty disc.  
57 The first demonstrated that nucleotomy of canine IVD increased the Range of Motion  
58 (ROM) and reduced disc height, whereas the presence of a hard mass inside the disc  
59 recovered the height loss but left ROM as wide as after nucleotomy [3]. The second  
60 attested that bone cement stabilized cervical discs, reducing the ROM compared to an  
61 intact spine [15]. Moreover, using animal surrogates usually limits access to naturally  
62 degenerated discs, consequently research has also focused on the best technique to  
63 model the vacuum phenomenon [16], [17], and the mechanical consequences of that  
64 surgery [18], [19]. In conclusion, PCD surgery relies on a weak knowledge of the  
65 mechanics of lumbar spine treated this way.

66 This study aims at enlarging knowledge about the mechanical consequences of PCD on  
67 lumbar spine stability. The motivations were two-fold: first, to develop a method to  
68 artificially represent a vacuum disc and the surgical technique applied to *in vitro*  
69 specimens, and to check the efficiency of this method as a model of PCD. Secondly, the  
70 study aimed at developing a methodology assessing the biomechanics of the spine before  
71 and after discoplasty. In particular, we hypothesized that PCD would recover the  
72 posterior disc height, affect the mechanical behaviour of the spine and present a damage  
73 risk for the surrounding tissue due to cement presence.

## 74 **2. MATERIALS AND METHODS**

### 75 **2.1. Specimens**

76 Ten functional spinal units were transected between T13 and L6 from porcine (*sus scrofa*  
77 *domesticus*) thoracolumbar spines. The animals were young and healthy porcine  
78 (approximately 9 months old and 100 kg) sacrificed for alimentary purposes. The  
79 specimens were cleaned using surgical tools: all soft tissues were carefully removed  
80 from the segment without damaging the vertebra, the facet joints and the intervertebral  
81 disc. In order to keep the natural kinetics of the segment while testing, the anterior,  
82 supraspinous and posterior ligaments were left intact. Each segment was aligned based  
83 on the disc orientation, using a six-degree-of-freedom clamp. Both segment extremities  
84 were potted with acrylic bone cement. Specimens were stored frozen at -20 °C between  
85 cleaning and testing phases and between the tests which has been proven not to affect  
86 significantly the segment biomechanics [20].

## 87 **2.2. Surgical procedure**

88 The purpose of the study is to develop a method to investigate the impact of PCD on the  
89 biomechanical behaviour of the spine by comparing IVD treated by this technique to  
90 degenerated and healthy IVDs. Thus, each specimen was tested in the three conditions  
91 sequentially:

- 92 • intact (INT) with a healthy IVD,
- 93 • after nucleotomy (NUCL) to simulate the instability of degenerated discs,
- 94 • after discoplasty (DP) (Fig. 1).

## 95 **2.3. Nucleotomy**

96 Since the porcine specimens were euthanized before reaching skeletal maturation,  
97 degenerated disc instability has been manually simulated by reproducing the vacuum  
98 inside of the disc. The specimens were thawed at room temperature. A square incision  
99 was performed with a scalpel blade in the annulus fibrosus on the latero-posterior side  
100 of the disc. The nucleus pulposus, easily identified due to its softness, was completely  
101 extracted through the excision with a curette. The endplates were shaved by scratching  
102 off the soft tissue until the surfaces felt smooth. This did not weaken the endplates, as  
103 no intravertebral leakage was observed during discoplasty. The size of the incision  
104 corresponded to the disc height. The specimens were frozen at -20 °C until testing.

## 105 **2.4. Discoplasty**

106 After being tested in degenerated conditions, the specimens were treated with  
107 discoplasty. For that, the specimens were thawed at room temperature. A high-viscosity  
108 radiopaque acrylic bone cement (10% BaSO<sub>4</sub>) (Tecres, Italy) was injected inside the  
109 disc through the incision. Because the empty IVD was no longer in tension, the segment  
110 was distracted/stretched during the injection to avoid an underestimation of the cement  
111 volume. After injection, the cement hardened for 30 min. The specimens were frozen at  
112 -20 °C until testing. In one specimen the facet joint was unintentionally damaged at the  
113 end of the last test: checking the test results in retrospect confirmed there was no artefact.

## 114 **2.5. Mechanical testing**

115 All the specimens underwent the same test conditions. In order to simulate *in vivo*  
116 kinetics of porcine spines, a load with offset was applied to simulate flexion, extension,

117 and lateral bending (the same side was selected for each specimen based on the possible  
118 damages made during the preparation). This simplified loading scenario was chosen as  
119 it allows reproducible simulation of a realistic loading scenario. In quadrupeds, the  
120 choice of a side is less significant than for humans since they do not have a predisposed  
121 limb side. The specimens were mechanically tested with a uniaxial servo-hydraulic  
122 testing machine (Mod. 8032, Instron, UK) operated in displacement control. The upper  
123 pot was rigidly fixed to the top of the testing machine while the other was loaded through  
124 a spherical joint moving along a rail (Fig. 1). Before testing, each specimen was thawed  
125 at room temperature and pre-conditioned applying a sinusoidal loading at 0.5 Hz for 20  
126 cycles to minimize viscoelastic creep effect. Specimens were loaded at 5.4 Nm by  
127 applying 200 N with an offset of 27 mm. The loading ramp lasted 1 s then the maximum  
128 loading was maintained for 0.3 s and the specimen was unloaded. The cycle was  
129 repeated 6 times (Fig. 2). Three cycles were found to be sufficient for preconditioning  
130 the data in another study [21], further cycles being nearly identical. The same trend was  
131 observed in these tests. The loading conditions were selected within the range of  
132 biological conditions, similar to other past studies [7], [14], [22]–[25]. Besides, the  
133 selected load avoided specimen damage. Each test was repeated twice to prove the  
134 experiment repeatability. Data extracted from the last cycle of both runs were averaged  
135 for each specimen. Axial load and displacement were acquired by the DIC system  
136 connected to a load cell (100 kN) at 15 Hz. Additionally, to have a more reliable  
137 sequence, the data were recorded with an independent computational unit (PXI,  
138 Labview, National Instruments, Aus. Texas, US) at 500 Hz. Unfortunately, some of the  
139 former records were missing for the first tests. Loads were either interpolated to have  
140 more data or smoothed with a median filter depending of the acquisition frequency.

## 141 **2.6. Displacement and strain with DIC**

142 For each test, the specimen surface has been studied using a Digital Image Correlation  
143 set-up in order to track its displacements and strains. This technique requires a high-  
144 contrast speckle pattern on the region of interest. Thus, a white-on-black speckle pattern  
145 was prepared on both the vertebra and the intervertebral disc (Fig. 1). First, the segment  
146 was stained 3 times with a methylene blue solution to create a dark background without  
147 impacting the properties of the tissues [26]. The white pattern was then sprayed  
148 following a procedure optimized elsewhere [27]. To measure the displacements and the  
149 deformations over the specimen surface, a 3D-DIC system (Q400, Dantec Dynamics,



150 Skovlunde, Denmark) and the associated software (Instron 4D, v.4.3.1, Dantec  
151 Dynamics) were used. Images were acquired by two cameras (5 Megapixels, 2440 x  
152 2050 pixels, 8-bit) with high-quality 35 mm lenses (Apo-Xenoplan 1.8/35, Schneider-  
153 Kreuznach, Bad-Kreuznach, Germany) inclined at an angle of 26° (white dot line on  
154 Fig. 1). The field of view covered the entire specimen (about 50mm by 30mm), which  
155 gave a pixel size of about 0.02mm. The specimen was lit by cold-light LEDs. Before the  
156 tests, calibration of the DIC system was performed using a dedicated target (A14-BMB-  
157 9x9, Dantec Dynamics). The parameters for the images acquisition and the correlation  
158 analysis have been previously optimized to minimize the error: facet size of 35 pixels,  
159 grid spacing of 11 pixels, and local filtering with a 7x7 pixels kernel. In order to  
160 investigate the biomechanical behaviour of the spine, two different acquisitions were  
161 performed:

- 162 • For extension and flexion: Lateral view of the segment with the cameras pointing  
163 at the neuroforamen
- 164 • For lateral bending; Frontal view of the specimen with the cameras pointing to  
165 the selected bending side

166 Images were taken at 15 Hz from the unloaded condition (reference frame, no load  
167 applied) to the end of the 6th cycle.

## 168 **2.7. Data analysis and statistics**

169 The parameters were extracted from the last load cycle of each of the two repetitions of  
170 each loading configuration. All measurements were compared for each specimen  
171 between the three disc conditions: intact, nucleotomy, discoplasty. In order to assess the  
172 changes in the nerve space in the neuroforamen, which is the main point in doing  
173 discoplasty, the posterior disc height was measured using DIC images: one point on each  
174 endplate was identified on the 3D profile of the disc in the back of the disc, close to the  
175 neuroforamen, where the nerve is passing. The points were aligned in the cranial-caudal  
176 direction. Their position was therefore tracked using DIC software. As a result, posterior  
177 disc height was only computed in flexion and extension, the frontal view not allowing  
178 height computation in lateral bending.

179 Displacements of the caudal vertebra in relation to the cranial vertebra were calculated  
180 from DIC images with a Matlab script. Assuming vertebra to be rigid bodies, the motions  
181 (translations and rotations) of each vertebra were computed based on singular value

182 decomposition. The ROM was defined as the relative angle between the vertebra in the  
183 sagittal plane between the peak load and unloaded conditions.

184 A pilot study of the load-displacement curves determined that, for porcine spines, the  
185 position having a first derivative of 30 N/mm was at the limit of the laxity zone (LZ).  
186 Stiffness was defined as the slope of load-displacement relationship in LZ. Although for  
187 some specimens this method underestimated the length of the LZ, the stiffness  
188 computation was not impacted since it was within the linear region [28].

189 All the computations were performed with dedicated Matlab scripts (Mathworks, Inc.,  
190 Natick, MA, USA). All height and strain measurements were evaluated by two  
191 independent observers. To limit inter-specimen variability influence, all stiffnesses,  
192 heights, and ROMs values were normalized to the intact condition.

193 In addition to posterior disc height, ROM, and stiffness calculations, the true principal  
194 strains over the specimen surface (vertebra and IVD) were measured at the peak load.  
195 In particular, the disc surface area was manually identified and the minimum, maximum  
196 and average of the first and second principal strains were extracted. Those measurements  
197 were performed in flexion and extension because the frontal view did not allow  
198 consideration of the neuroforamen area.

199 For each parameter, outlying data were preliminarily tested and excluded using the  
200 Peirce criterion [29], this resulted in a 10% data exclusion at the maximum. Test  
201 parameters were computed based on the sixth cycle. Mean  $\pm$  standard deviation of all  
202 the outcomes were calculated and presented by group. Due to the small specimen  
203 number, comparisons between the three conditions were made for ROM, stiffness,  
204 height, and the strain average with a non-parametric test (Wilcoxon's sign rank, with  
205 Matlab).

## 206 **2.8. Cement distribution**

207 In order to study the cement distribution inside of the disc, scans of the specimens have  
208 been performed after discoplasty with a clinical computed tomography scanner  
209 (Aquilion ONE, Toshiba) with 120 mA, 135 kV and a 0.5 mm voxel. The scans of nine  
210 specimens out of ten were available due to a practical mistake. The shape of the cement,  
211 its capacity to fill the disc cavity, the endplates and AF contact were visually assessed  
212 by a spine surgeon (P.E.) from the 3D reconstruction of the PMMA geometry.  
213 Segmentation process was performed in Mimics® image analysis software (Mimics

214 Research, Mimics Innovation Suite v21.0, Materialise, Leuven, Belgium) on the 2D CT  
215 images using thresholding algorithm.

## 216 **3. RESULTS**

### 217 **3.1. Posterior disc height**

218 The posterior disc height was measured in the three conditions. At peak load, intact  
219 posterior disc height was higher in flexion than in extension. Nucleotomy significantly  
220 decreased the posterior height for both flexion ( $p=0.006$ , Wilcoxon) and extension  
221 ( $p=0.049$ , Wilcoxon) (Fig. 3). On the contrary, discoplasty restored the height. Results  
222 were normalized to the initial posterior height for each specimen. In extension, height  
223 after discoplasty was significantly higher (105% of the intact height) than after  
224 nucleotomy (81%) ( $p= 0.04$ , Wilcoxon). In flexion, posterior disc height was  
225 respectively 84% and 94% of the intact height after nucleotomy and discoplasty but the  
226 difference between the two conditions was not significant ( $p=0.11$ , Wilcoxon).

### 227 **3.2. Range of motion**

228 Intervertebral motions in the applied direction were one order of magnitude higher  
229 compared to the other directions. Only the motions in the applied direction are reported  
230 here. In flexion and lateral bending, nucleotomy reduced the ROM (Fig. 4). The ROM  
231 in extension slightly increased after nucleotomy and discoplasty compared to the intact  
232 condition. The results for degenerated and discoplasty discs were normalized by the  
233 intact ROM for each motion. ROM was not significantly different between nucleotomy  
234 and discoplasty in flexion (Wilcoxon sign-rank test,  $p=0.57$ ), extension ( $p=0.43$ ) and  
235 lateral bending ( $p=0.50$ , Wilcoxon).

### 236 **3.3. Stiffness**

237 Stiffness was computed for only 9 out of 10 specimens due to a technical problem during  
238 acquisition. Specimens had very different behaviours regardless of the loading  
239 configuration and spinal level. The majority of the tests presented a “toe-region” before  
240 a stiff region. A recovery after discoplasty of the initial behaviour compared to after  
241 nucleotomy was also observed (Fig. 5). The results for nucleotomy and discoplasty discs  
242 were normalized by the intact stiffness for each loading configuration. Stiffness was not

243 significantly different after nucleotomy and discoplasty in flexion ( $p=0.47$ , Wilcoxon),  
244 extension ( $p=0.95$ , Wilcoxon) and lateral bending ( $p=0.46$ , Wilcoxon) (Fig. 6).

### 245 **3.4. Strain distribution**

246 DIC correlation has been successfully performed in flexion and extension only because  
247 the frontal view did not allow all of the disc surface to be captured. First of all, bone  
248 strains were in a  $[-1.5\%, 1.5\%]$  range on the vertebra surface whereas they reached  $-17\%$   
249 and  $+11\%$  on the discs. Moreover, IVD principal strains presented different behaviours  
250 depending on the loading configuration (Fig. 7). In flexion, for all disc conditions, the  
251 highest values of compressive strain are located at the cranial and caudal extremities of  
252 the IVD, starting from the anterior and spreading toward the posterior along the  
253 endplates. After nucleotomy and discoplasty, the trend was more pronounced. However,  
254 cemented discs presented lower values in this area than empty discs. The highest values  
255 of tensile principal strain were in the centre of the IVD with peak  $>3\%$  of strain in the  
256 posterior region. In extension, tensile strains were larger in the anterior of the disc while  
257 high compressive strains were located in the posterior area of the disc. Discoplasty  
258 reduced the strains in most of the disc, whereas for intact and nucleotomy, high strains  
259 were found on the whole disc.

260 Nucleotomy seems to have a greater effect on the compressive strain in flexion and  
261 extension (Table 1). Meanwhile, discoplasty halved the average tensile strain of disc  
262 surface compared to nucleotomy condition in extension ( $p=0.0195$ , Wilcoxon) but had  
263 similar values of second principal strain. Regarding the peak strains, discoplasty only  
264 presented a value larger than intact condition for extension. Other extreme strains were  
265 observed after nucleotomy although the differences were not significant.

### 266 **3.5. Cement distribution**

267 Nine specimens have been scanned to control cement distribution within the discs.  
268 Visual assessment of the specimen scans focused on the position of the cement mass  
269 within the intervertebral disc in the sagittal and frontal planes, whether it was in contact  
270 with endplates and AF, the shape of the distribution, and the ratio of disc filling. The  
271 majority of specimens had a cement volume located in the posterior of the disc (9/9  
272 specimens), centred in the lateral direction (8/9 specimens), in contact with the endplates

273 (8/9). Only two specimens did not present contact between the cement and the AF (Fig.  
274 8). The NP cavity was fully filled with cement in 5 specimens, three discs were almost  
275 filled at >80% of the NP volume, and one at less than 80%. Among the specimens, seven  
276 were validated by a clinician as discoplasty models compared to cement distribution  
277 after human surgery taking porcine anatomical specificities into account, and two were  
278 sub-optimal (Fig. 9). No outlier corresponded to the sub-optimal cemented specimens.  
279 All specimens presented a smaller cement volume than in human surgery (Table 2).

#### 280 **4. DISCUSSION**

281 According to clinical observations [11], a loss of disc height due to disc degeneration  
282 would result in a reduction of the neuroforamen where the back nerves are passing,  
283 compressing them and creating pain for the patient. This animal *in vitro* study aimed at  
284 exploring the feasibility of assessing the mechanical consequences on spine stability  
285 after discoplasty surgical procedure. An *in vitro* experiment was successfully conducted  
286 to establish posterior disc height, ROM, stiffness, and strains over porcine specimen  
287 surfaces.

288 After nucleotomy a decrease of the posterior disc height of 15% was measured. This  
289 result validated such *in vitro* nucleotomy as a simulation of degenerated disc.  
290 Furthermore, nucleotomy was associated with a decrease of ROM (not statistically  
291 significant in our sample). After discoplasty, the injected cement acted like a spacer  
292 resulting in a significant recovery of the posterior height (105% of the intact height in  
293 extension). This trend supported the clinical observations [11] and confirmed that PCD  
294 recovered the disc height and enlarged neuroforamen space, which is the main objective  
295 of this surgery. ROM and stiffness did not show any significant difference between the  
296 degenerated and treated cases for any loading. Thus, discoplasty did not significantly  
297 impact spine flexibility in this experimental setup.

298 To the authors' knowledge, this was the first study addressing the consequences of  
299 discoplasty on the distribution of strain on the disc surface. The strain distribution  
300 measured after nucleotomy showed a specific pattern with intense regions, while  
301 discoplasty reduced this abnormal distribution with more moderate strain values.

302 DIC results showing the AF principal strains can be related to the ROM and the posterior  
303 disc height. After nucleotomy, because of the reduced posterior height and because the  
304 annulus is no longer constrained from inside, the annulus fibres bulged more, leading to

305 intense tensile strains at the apex of the bulging. At the same time, this more pronounced  
306 bulging at mid-height caused a more pronounced concavity at the disc cranial and caudal  
307 extremities, which led to larger compressive strains in this region. After discolplasty, the  
308 injected cement spaced the endplates, and even if the cement did not stretch radially the  
309 disc fibres as the NP would do, the overall bulging was more limited, and less intense  
310 tensile strains were measured. As the cement acts as a very stiff spacer, very small strains  
311 were visible in most of the disc surface, the only highly strained region in the disc was  
312 near the endplates. Strain values after discolplasty did not exceed what the endplates  
313 underwent in nucleotomy condition. If the specimen endplates presented any weakness,  
314 this could lead to long-term damages due to the load concentration. The peak strain  
315 values increased after nucleotomy, and decreased again after cement injection, reaching  
316 intact-like values. No correlation between the strain peaks on the specimen surface and  
317 the cement distribution assessed from the CT scans was found. Even in the specimens  
318 where contact between the AF and the cement was noted, this did not result in a specific  
319 strain distribution.

320 The ROM measured at peak load was in the same range as other *in vitro* studies on  
321 porcine lumbar spines [22], [30]. Others studies investigating the effect of nucleotomy  
322 demonstrated that the absence of NP reduced segmental rotational stability, significantly  
323 increasing the ROM [14], [19], [23].

324 Discoplasty being a recent surgical technique, the authors found only one article  
325 applying a similar surgery, on dog cervical discs [3]: nucleotomy was also performed  
326 through an AF fenestration and a spacer implant was inserted. Similar to the present  
327 study, Moissonier *et al* found that nucleotomy completely disrupted spine stability,  
328 increasing significantly the ROM. Both the spacer used in their study, and the cement  
329 injected in ours failed to recover disc mobility. Similarly, the cement set in the cervical  
330 disc by Wilke *et al* reduced the ROM compared to intact disc condition. However, this  
331 study tested bone cement to anticipate interbody fusion, and the AF was not fully intact  
332 [15]. This was the major difference with soft disc filler materials which are more likely  
333 to restore intact ROM as well [14].

334 Although the results were normalized with respect to the intact to integrate the specimen  
335 anatomical specificity, and one outlier was removed, inter-specimen variability  
336 remained large, with no correlation with the segment level. Our tests differed from most  
337 of the literature [28] as the FSUs were tested separately in flexion and extension,  
338 therefore direct comparisons of the stiffness are not possible.

339 This study aimed to start exploring the biomechanical effects of discoplasty. Since this  
340 is a preliminary study, an animal model was more justifiable for ethical reasons. The  
341 use of breed porcine rather than human spines was preferred as they have less inter-  
342 specimen variation of anatomy and mechanical properties. Indeed, porcine models are  
343 commonly used to replicate human spine surgeries [31], [32]. Porcine spines could be  
344 good surrogates for *in vitro* testing, even if they exhibit larger ROM and lower stiffness  
345 [33]–[35]. Since the porcine specimens were obtained before reaching skeletal maturity,  
346 finding IVDs presenting a similar degenerated level with a vacuum as required for PCD  
347 was impossible. Nucleotomy did not aim at modelling a degenerated disc state but at  
348 creating the spine instability observed clinically based on the disc vacuum. Porcine  
349 results should therefore be qualitatively extrapolated to humans in terms of trends rather  
350 than interpreting absolute values as this study aimed at.

351 Vacuum volume has not been measured in this study. The importance of this parameter  
352 is unclear in the clinical practice. A recent study investigating the Vacuum Phenomenon  
353 (VP) impact for PCD indication concluded that the volume of vacuum could not be used  
354 as a proper indication for this surgery [36]. Moreover, during the PCD procedure, the  
355 patient position aims at enlarging the intervertebral space by reducing the segmental  
356 lordosis. Thus, the volume of the empty disc available during the surgery is larger than  
357 the VP computed on imaging.

358 Usual methods to measure the disc height like Farfan or Frobin were not applied here to  
359 assess the intervertebral space. Indeed, these methods were conceived for clinical  
360 application considering the vertical height along the antero-posterior disc length on  
361 medical images, taking account of the whole disc and its orientation. This study,  
362 however, focused on the nerve space within the neuroforamen. Only the volume where  
363 the nerve passed was critical, based on clinical observations, and the discoplasty surgery  
364 was applied in first approach to re-open the foramen space by achieving indirect  
365 decompression. That is why a comparative study has been performed selecting two  
366 points at the endplates level the closest from the neuroforamen, rather than relying on a  
367 more general measurement of the disc height. The study concentrated on parameters  
368 with meaning for the clinical purpose of the surgery. Moreover, the most critical case  
369 was also investigated: physiologically when the disc is loaded in extension and the  
370 neuroforamen is the most reduced. So, measurements at the peak load were more  
371 interesting for the study.

372 The impact of AF fenestration during nucleotomy on the segment stability has not been  
373 assessed here, however Michalek *et al* reported alterations of IVD mechanics with disc  
374 height loss under a compressive load, following different types of incisions [37]. Disc  
375 lesions were also found to reduce the peak moment depending on the damage shape [38].  
376 As a consequence, our study may overestimate motion range. However, it was  
377 hypothesized that the lack of NP would destabilize the segment in larger proportion than  
378 the fenestration of AF.

379 Pure moment is the gold-standard loading for *in vitro* spine testing in a relevant bending  
380 condition. For spine segments consisting of several vertebrae, bending is usually  
381 associated with a follower load equipment to model the *in vivo* kinematics, including the  
382 effect of the muscles adding a compressive loading [39], [40]. Similarly, a compressive  
383 preload is found in a single FSU, but in this case a follower load cannot be implemented.  
384 In this study, an alternative loading configuration was chosen to ensure that reproducible  
385 testing conditions could be applied, thus allowing the comparison of the biomechanics  
386 of a specimen tested at different times with each of the different disc conditions. The  
387 load applied here was a combination of axial compression and bending, an alternative  
388 loading to pure bending of the spine [26], [41]–[44]. It has been demonstrated that  
389 without preload, *in vivo* stiffness of the spine segment was underestimated applying pure  
390 bending [45]. In our study, the combination of axial compression and bending allowed  
391 a more physiological spine loading with an axial component which substitutes of the  
392 preload.

## 393 **5. CONCLUSION**

394 So far, the only knowledge about PCD comes from clinical experience on few cases.  
395 This paper presents a feasibility study, to develop a test model and perform a preliminary  
396 investigation on the biomechanics of PCD. The study also aimed at analyzing and  
397 verifying if there is any clear mechanical risk associated with injection of cement in the  
398 cavity of a disc. No specific clinical recommendations (e.g. indication for specific  
399 patient groups) can be directly obtained from the present study. This study aimed at  
400 developing an *in vitro* surrogate to test a highly degenerated disc with vacuum inside,  
401 and to assess the biomechanical changes related to discoplasty in porcine spines. The  
402 main conclusions could be summarized in key points.



- 403 • The *in vitro* method was successfully developed to model nucleotomy.
- 404 • The *in vitro* testing protocol applied to discoplasty allowed to measure the effect  
405 of this minimally invasive surgery on the spine biomechanics.
- 406 • Nucleotomy decreased the posterior disc height. Discoplasty restored the height  
407 significantly, maintaining a gap between the vertebral bodies and re-opening the  
408 neuroforamen area as observed in clinical practice.
- 409 • The CT scans confirmed that the distribution of the cement had a similar  
410 distribution inside the disc for most specimens compared to human post-surgery  
411 observations, although the cavity after nucleotomy and the cement volume were  
412 smaller than in human cases.
- 413 • Discoplasty did not impact the ROM nor the stiffness, which remained similar  
414 to the nucleotomy condition because the cement did not directly interact with the  
415 AF nor the facets.
- 416 • Discoplasty concentrated the strains along the endplates, reducing the strain  
417 value on the middle of the disc. The average strain over the disc was decreased  
418 after discoplasty compared to nucleotomy, limiting the risks of fibre tears.
- 419 • The goal of this preliminary study on a limited number of porcine specimens was  
420 to establish trends which could justify a larger study on human specimens.

## 421 **Acknowledgments**

422 The Authors wish to thank Federico Morosato from the University of Bologna for  
423 providing the Matlab scripts.

424 Villalba Hospital is acknowledged for hosting the scan sessions; special thanks to  
425 Pierangela Moro for the skilled advice and for her great patience.

426 Special thanks are expressed to Cameron James, ESR within the Spinner project, for  
427 proof-reading the manuscript.

428 The use Mimics Software was possible thanks to the Hungarian Scientific Research  
429 Fund (OTKA FK123884).

430 This project was founded by European Union's Horizon 2020 Marie Skłodowska-Curie  
431 ITN grant SPINNER No. 766012.

432 **Conflict of interest statement**

433 There is no potential conflict of interest: none of the Authors received or will receive  
434 direct or indirect benefits from third parties for the performance of this study.

435

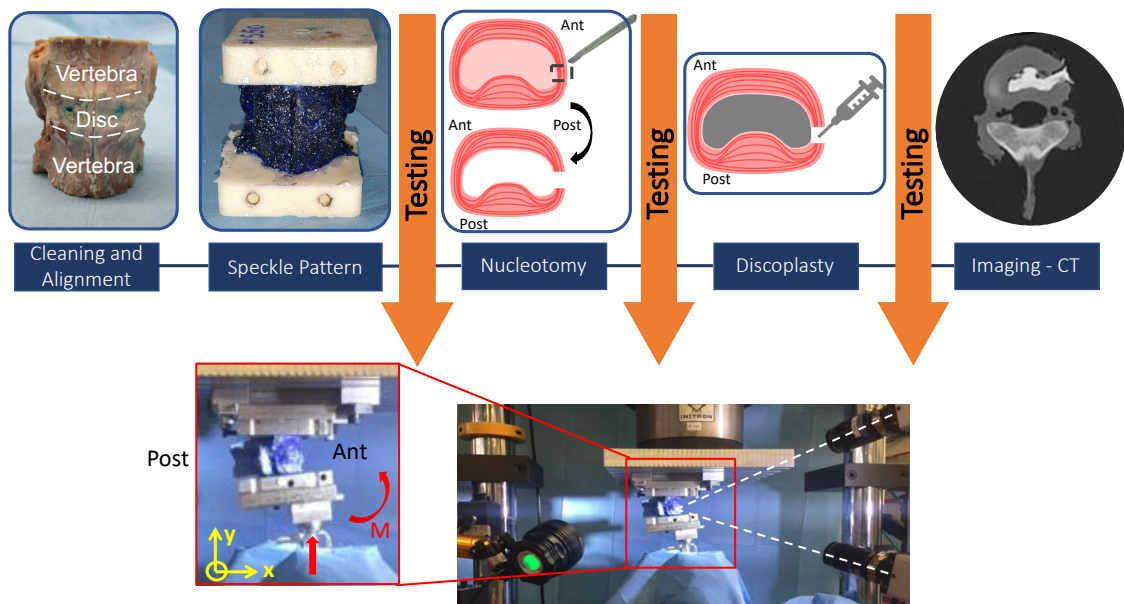
- 437 [1] « 6. Priority diseases and reasons for inclusion », in *WHO | Priority Medicines*  
438 *for Europe and the World Update Report*, 2013.
- 439 [2] I. Oda, K. Abumi, B.-S. Yu, H. Sudo, et A. Minami, « Types of Spinal Instability  
440 That Require Interbody Support in Posterior Lumbar Reconstruction: An In Vitro  
441 Biomechanical Investigation. [Miscellaneous Article] », *Spine*, vol. 28, n° 14, p.  
442 1573-1580, juill. 2003.
- 443 [3] P. Moissonnier, L. Desquilbet, D. Fitzpatrick, et F. Bernard, « Radiography and  
444 biomechanics of sixth and seventh cervical vertebrae segments after disc  
445 fenestration and after insertion of an intervertebral body spacer », *Vet. Comp.*  
446 *Orthop. Traumatol.*, vol. 27, n° 1, p. 54-61, 2014, doi: 10.3415/VCOT-11-11-  
447 0159.
- 448 [4] X. Li, Y. Song, et H. Duan, « Reconstruction of Segmental Stability of Goat  
449 Cervical Spine with Poly (D, L-lactic acid) Cage », *Orthop. Surg.*, vol. 7, n° 3, p.  
450 266-272, 2015, doi: 10.1111/os.12192.
- 451 [5] F. Kandziora, R. Pflugmacher, M. Scholz, T. D. Eindorf, K. J. Schnake, et N. P.  
452 Haas, « Bioabsorbable Interbody Cages in a Sheep Cervical Spine Fusion  
453 Model. », *Spine*, vol. 29, n° 17, p. 1845-1855, sept. 2004.
- 454 [6] F. Kandziora *et al.*, « Comparison of BMP-2 and combined IGF-I/TGF- $\beta$ 1  
455 application in a sheep cervical spine fusion model », *Eur. Spine J.*, vol. 11, n° 5,  
456 p. 482-493, oct. 2002, doi: 10.1007/s00586-001-0384-4.
- 457 [7] Y. Gu, Z. Yao, L. Jia, J. Qi, et J. Wang, « In vivo experimental study of hat type  
458 cervical intervertebral fusion cage (HCIFC) », *Int. Orthop.*, vol. 34, n° 8, p.  
459 1251-1259, déc. 2010, doi: 10.1007/s00264-010-0978-8.
- 460 [8] Z. Chunguang *et al.*, « Evaluation of Bioabsorbable Multiamino Acid  
461 Copolymer/ $\alpha$ -Tri-Calcium Phosphate Interbody Fusion Cages in a Goat Model »,  
462 *Spine*, vol. 36, n° 25, p. E1615-E1622, déc. 2011, doi:  
463 10.1097/BRS.0b013e318210ca32.
- 464 [9] M. J. Allen, Y. Hai, N. R. Ordway, C.-K. Park, B. Bai, et H. A. Yuan,  
465 « Assessment of a synthetic anterior cervical ligament in a spinal fusion model in  
466 sheep », *Spine J.*, vol. 2, n° 4, p. 261-266, juill. 2002, doi: 10.1016/S1529-  
467 9430(02)00188-2.
- 468 [10] S. E. Emery, D. A. Fuller, et S. D. Stevenson, « Ceramic Anterior Spinal Fusion:  
469 Biologic and Biomechanical Comparison in a Canine Model. [Miscellaneous  
470 Article] », *Spine*, vol. 21, n° 23, p. 2713-2719, déc. 1996.
- 471 [11] P. P. Varga, G. Jakab, I. B. Bors, A. Lazary, et Z. Szövérfi, « Experiences with  
472 PMMA cement as a stand-alone intervertebral spacer », *Orthop.*, vol. 44, n° 1, p.  
473 1-8, nov. 2015, doi: 10.1007/s00132-014-3060-1.
- 474 [12] C. Sola *et al.*, « Percutaneous cement discoplasty for the treatment of advanced  
475 degenerative disk disease in elderly patients », *Eur. Spine J.*, mars 2018, doi:  
476 10.1007/s00586-018-5547-7.
- 477 [13] L. Kiss, P. P. Varga, Z. Szoverfi, G. Jakab, P. E. Eltes, et A. Lazary, « Indirect  
478 foraminal decompression and improvement in the lumbar alignment after  
479 percutaneous cement discoplasty », *Eur. Spine J.*, avr. 2019, doi:  
480 10.1007/s00586-019-05966-7.
- 481 [14] H.-J. Wilke, F. Heuer, C. Neidlinger-Wilke, et L. Claes, « Is a collagen scaffold  
482 for a tissue engineered nucleus replacement capable of restoring disc height and  
483 stability in an animal model? », *Eur. Spine J.*, vol. 15, n° 3, p. 433-438, août  
484 2006, doi: 10.1007/s00586-006-0177-x.

- 485 [15] H.-J. Wilke, A. Kettler, et L. Claes, « Primary stabilizing effect of interbody  
486 fusion devices for the cervical spine: an in vitro comparison between three  
487 different cage types and bone cement », *Eur. Spine J.*, vol. 9, n° 5, p. 410-416,  
488 oct. 2000, doi: 10.1007/s005860000168.
- 489 [16] G. Vadalà *et al.*, « A Nucleotomy Model with Intact Annulus Fibrosus to Test  
490 Intervertebral Disc Regeneration Strategies », *Tissue Eng. Part C Methods*, vol.  
491 21, n° 11, p. 1117-1124, 2015, doi: <http://dx.doi.org/10.1089/ten.tec.2015.0086>.
- 492 [17] G. Vadalà *et al.*, « The Transpedicular Approach As an Alternative Route for  
493 Intervertebral Disc Regeneration »:, *Spine*, vol. 38, n° 6, p. E319-E324, mars  
494 2013, doi: 10.1097/BRS.0b013e318285bc4a.
- 495 [18] M. Shea, T. Y. Takeuchi, R. H. Wittenberg, A. A. White, et W. C. Hayes, « A  
496 Comparison of the Effects of Automated Percutaneous Discectomy and  
497 Conventional Discectomy on Intradiscal Pressure, Disk Geometry, and  
498 Stiffness »:, *J. Spinal Disord.*, vol. 7, n° 4, p. 317-325, août 1994, doi:  
499 10.1097/00002517-199408000-00005.
- 500 [19] W. Johannessen, J. M. Cloyd, G. D. O'Connell, E. J. Vresilovic, et D. M. Elliott,  
501 « Trans-Endplate Nucleotomy Increases Deformation and Creep Response in  
502 Axial Loading », *Ann. Biomed. Eng.*, vol. 34, n° 4, p. 687-696, avr. 2006, doi:  
503 10.1007/s10439-005-9070-8.
- 504 [20] J. S. Tan et S. Uppuganti, « Cumulative Multiple Freeze-Thaw Cycles and  
505 Testing Does Not Affect Subsequent Within-Day Variation in Intervertebral  
506 Flexibility of Human Cadaveric Lumbosacral Spine », *SPINE*, vol. 37, n° 20, p.  
507 E1238-E1242, 2012.
- 508 [21] J. M. Cottrell, M. C. H. van der Meulen, J. M. Lane, et E. R. Myers, « Assessing  
509 the Stiffness of Spinal Fusion in Animal Models », *HSS J.*, vol. 2, n° 1, p. 12-18,  
510 févr. 2006, doi: 10.1007/s11420-005-5123-7.
- 511 [22] J. P. Dickey et D. J. Kerr, « Effect of specimen length: are the mechanics of  
512 individual motion segments comparable in functional spinal units and  
513 multisegment specimens? », *Med. Eng. Phys.*, vol. 25, n° 3, p. 221-227, avr.  
514 2003, doi: 10.1016/S1350-4533(02)00152-2.
- 515 [23] F. Russo *et al.*, « Biomechanical Evaluation of Transpedicular Nucleotomy With  
516 Intact Annulus Fibrosus »:, *SPINE*, vol. 42, n° 4, p. E193-E201, févr. 2017, doi:  
517 10.1097/BRS.0000000000001762.
- 518 [24] D. J. Sucato, « Thoracoscopic Discectomy and Fusion in an Animal Model: Safe  
519 and Effective When Segmental Blood Vessels Are Spared. », *SPINE*, vol. 27, n°  
520 8, p. 880-886, 2002.
- 521 [25] Chung et Teoh, « Multi-axial Spine Biomechanical Testing System with Speckle  
522 Displacement Instrumentation », *J. Biomech. Eng.*, vol. 124, n° 4, p. 471-477,  
523 août 2002, doi: 10.1115/1.1493803.
- 524 [26] M. Palanca, M. Marco, M. L. Ruspi, et L. Cristofolini, « Full-field strain  
525 distribution in multi-vertebra spine segments: An in vitro application of digital  
526 image correlation », *Med. Eng. Phys.*, vol. 52, p. 76-83, févr. 2018, doi:  
527 10.1016/j.medengphy.2017.11.003.
- 528 [27] M. Palanca, T. M. Brugo, et L. Cristofolini, « USE OF DIGITAL IMAGE  
529 CORRELATION TO INVESTIGATE THE BIOMECHANICS OF THE  
530 VERTEBRA », *J. Mech. Med. Biol.*, vol. 15, n° 02, p. 1540004, avr. 2015, doi:  
531 10.1142/S0219519415400047.
- 532 [28] H.-J. Wilke, K. Wenger, et L. Claes, « Testing criteria for spinal implants:  
533 recommendations for the standardization of in vitro stability testing of spinal

- 534 implants », *Eur. Spine J.*, vol. 7, n° 2, p. 148-154, mai 1998, doi:  
535 10.1007/s005860050045.
- 536 [29] S. M. Ross, « Peirce's criterion for the elimination of suspect experimental  
537 data », *J. Eng. Technol.*, p. 1-12, 2003.
- 538 [30] J. T. Lysack, J. P. Dickey, G. A. Dumas, et D. Yen, « A continuous pure moment  
539 loading apparatus for biomechanical testing of multi-segment spine specimens »,  
540 *J. Biomech.*, vol. 33, n° 6, p. 765-770, juin 2000, doi: 10.1016/S0021-  
541 9290(00)00021-X.
- 542 [31] Busscher, « Comparative anatomical dimensions of the complete human and  
543 porcine spine », 2010.
- 544 [32] C. Daly, P. Ghosh, G. Jenkin, D. Oehme, et T. Goldschlager, « A Review of  
545 Animal Models of Intervertebral Disc Degeneration: Pathophysiology,  
546 Regeneration, and Translation to the Clinic », *BioMed Res. Int.*, vol. 2016, 2016,  
547 doi: 10.1155/2016/5952165.
- 548 [33] H.-J. Wilke, J. Geppert, et A. Kienle, « Biomechanical in vitro evaluation of the  
549 complete porcine spine in comparison with data of the human spine », *Eur. Spine  
550 J.*, vol. 20, n° 11, p. 1859-1868, nov. 2011, doi: 10.1007/s00586-011-1822-6.
- 551 [34] J. P. Dickey, G. A. Dumas, et D. A. Bednar, « Comparison of porcine and human  
552 lumbar spine flexion mechanics\* », *Vet. Comp. Orthop. Traumatol.*, vol. 16, n°  
553 01, p. 44-49, 2003, doi: 10.1055/s-0038-1632753.
- 554 [35] I. Busscher, A. J. van der Veen, J. H. van Dieen, I. Kingma, G. J. Verkerke, et A.  
555 G. Veldhuizen, « In Vitro Biomechanical Characteristics of the Spine A  
556 Comparison Between Human and Porcine Spinal Segments », *SPINE*, vol. 35, n°  
557 2, p. E35-E42, janv. 2010, doi: 10.1097/BRS.0b013e3181b21885.
- 558 [36] G. Camino Willhuber *et al.*, « Development of a New Therapy-Oriented  
559 Classification of Intervertebral Vacuum Phenomenon With Evaluation of Intra-  
560 and Interobserver Reliabilities », *Glob. Spine J.*, p. 2192568220913006, mars  
561 2020, doi: 10.1177/2192568220913006.
- 562 [37] A. J. Michalek et J. C. Iatridis, « Height and torsional stiffness are most sensitive  
563 to annular injury in large animal intervertebral discs », *Spine J.*, vol. 12, n° 5, p.  
564 425-432, mai 2012, doi: 10.1016/j.spinee.2012.04.001.
- 565 [38] R. E. Thompson, M. J. Percy, et T. M. Barker, « The mechanical effects of  
566 intervertebral disc lesions », *Clin. Biomech.*, vol. 19, n° 5, p. 448-455, juin 2004,  
567 doi: 10.1016/j.clinbiomech.2004.01.012.
- 568 [39] A. G. Patwardhan, R. M. Havey, K. P. Meade, B. Lee, et B. Dunlap, « A  
569 Follower Load Increases the Load-Carrying Capacity of the Lumbar Spine in  
570 Compression. », *SPINE*, vol. 24, n° 10, p. 1003-1009, 1999.
- 571 [40] A. G. Patwardhan, K. P. Meade, et B. Lee, « A Frontal Plane Model of the  
572 Lumbar Spine Subjected to a Follower Load: Implications for the Role of  
573 Muscles », *J. Biomech. Eng.*, vol. 123, n° 3, p. 212-217, juin 2001, doi:  
574 10.1115/1.1372699.
- 575 [41] M. A. Adams, S. May, B. J. C. Freeman, H. P. Morrison, et P. Dolan, « Effects of  
576 Backward Bending on Lumbar Intervertebral Discs: Relevance to Physical  
577 Therapy Treatments for Low Back Pain. », *SPINE*, vol. 25, n° 4, p. 431-437,  
578 2000.
- 579 [42] M. Al-Rawahi, J. Luo, P. Pollintine, P. Dolan, et M. A. Adams, « Mechanical  
580 Function of Vertebral Body Osteophytes, as Revealed by Experiments on  
581 Cadaveric Spines »:, *Spine*, vol. 36, n° 10, p. 770-777, mai 2011, doi:  
582 10.1097/BRS.0b013e3181df1a70.

- 583 [43] M. L. Ruspi, M. Palanca, C. Faldini, et L. Cristofolini, « Full-field in vitro  
584 investigation of hard and soft tissue strain in the spine by means of Digital Image  
585 Correlation », *Muscles Ligaments Tendons J.*, vol. 7, n° 4, p. 538-545, avr. 2018,  
586 doi: 10.11138/mltj/2017.7.4.538.
- 587 [44] M. Adams et P. Dolan, « Time-dependent changes in the lumbar spine's  
588 resistancce to bending », *Clin. Biomech.*, vol. 11, n° 4, p. 194-200, juin 1996, doi:  
589 10.1016/0268-0033(96)00002-2.
- 590 [45] M. G. Gardner-Morse et I. A. Stokes, « Physiological axial compressive preloads  
591 increase motion segment stiffness, linearity and hysteresis in all six degrees of  
592 freedom for small displacements about the neutral posture », *J. Orthop. Res.*, vol.  
593 21, n° 3, p. 547-552, janv. 2003, doi: 10.1016/S0736-0266(02)00199-7.  
594  
595

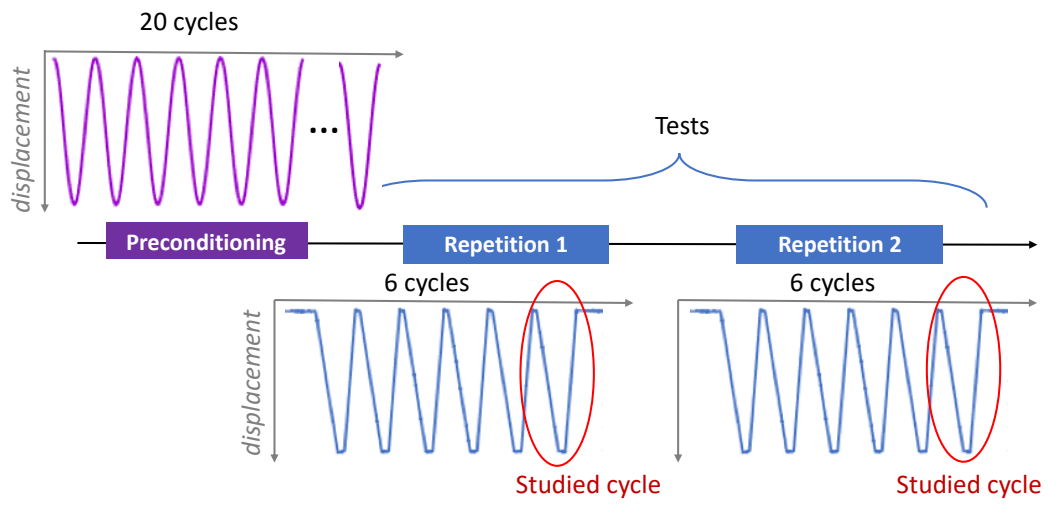
596 CAPTIONS TO FIGURES



597  
598  
599

**Fig. 1** – Experimental workflow of the study. The arrow represents the applied load and the resulting moment  $M$ .

600

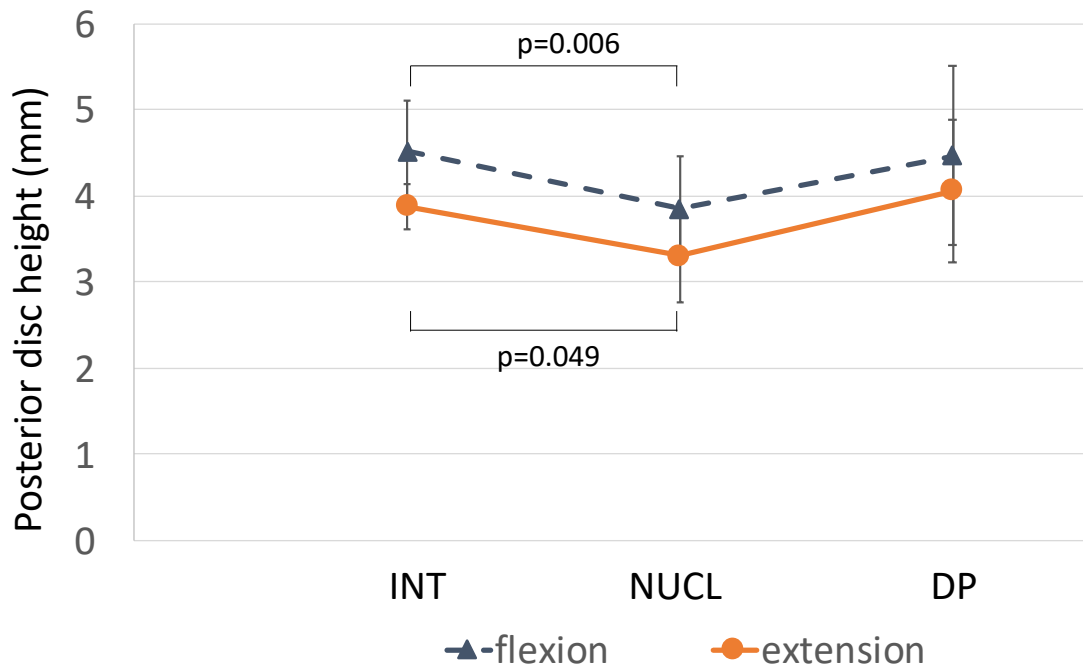


601

602 **Fig. 2** – Workflow of the applied displacement for flexion, extension, and lateral  
603 bending.



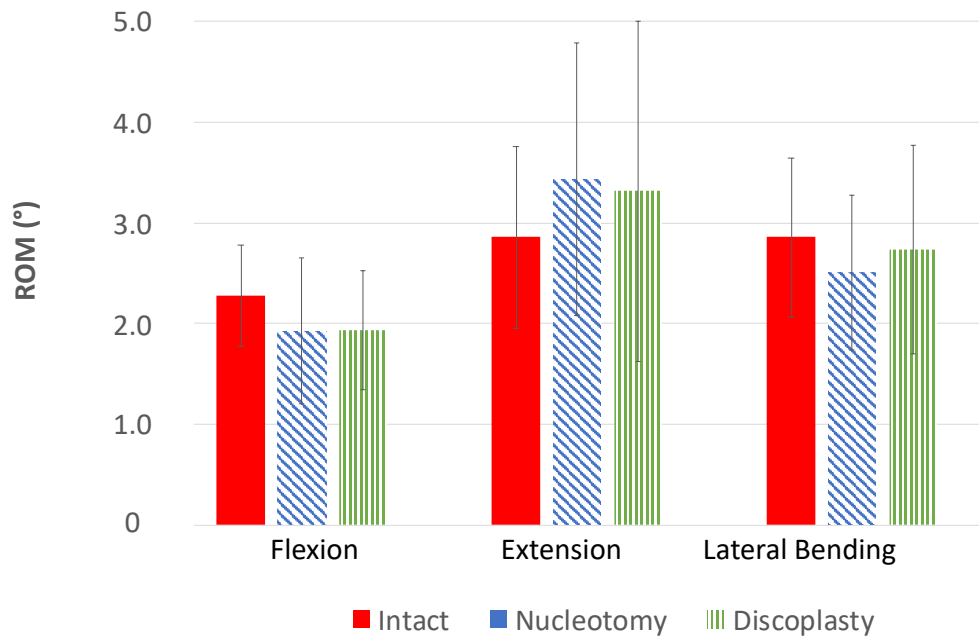
604



605

606 **Fig. 3** – Intervertebral posterior disc height recorded at the peak load in intact  
607 condition, after nucleotomy, and discoplasty for both motions. Average over all  
608 specimens and standard deviation were represented (n=10). Normalized data showed  
609 significant differences in flexion (p=0.11) and extension (p=0.04) between NUCL and  
610 DP.

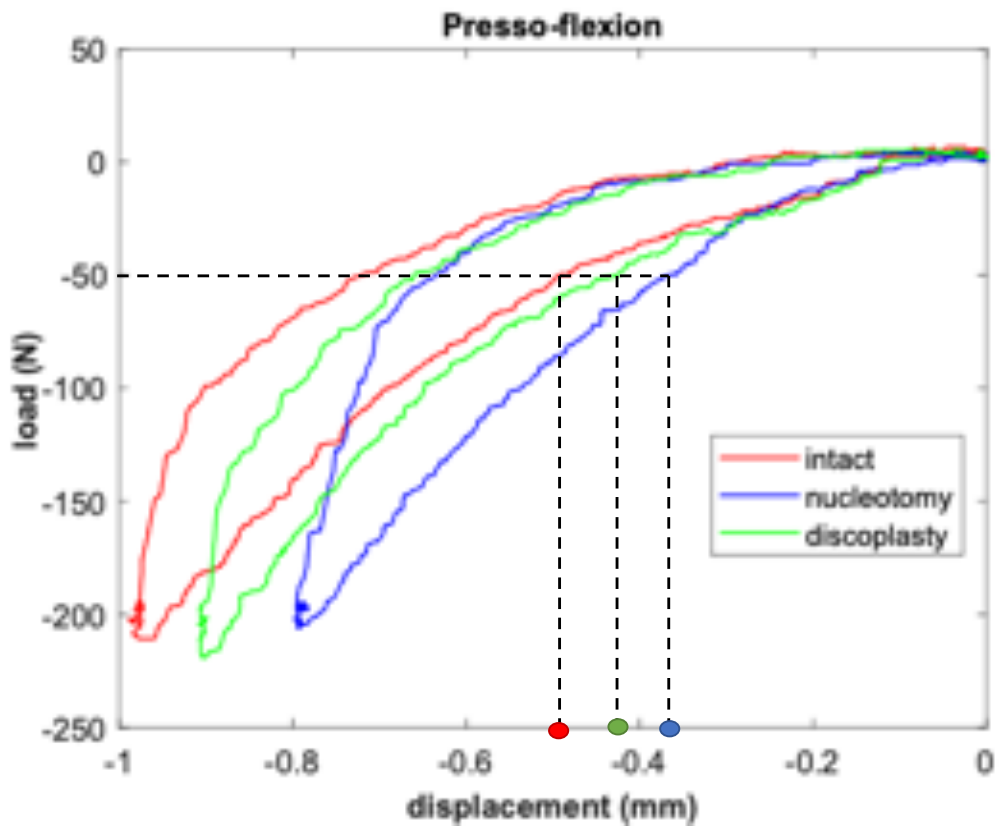
611



612

613 **Fig. 4** – Range of Motion recorded at peak load for flexion, extension and lateral  
614 bending, in all disc conditions. Normalized data were not statistically significant  
615 ( $p>0.1$ ).

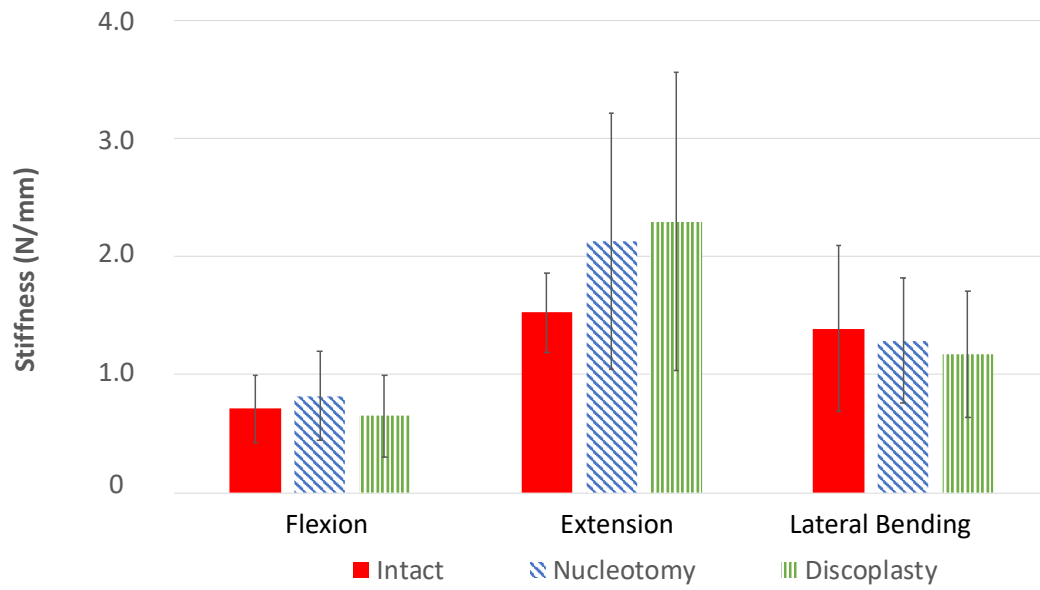
616



617

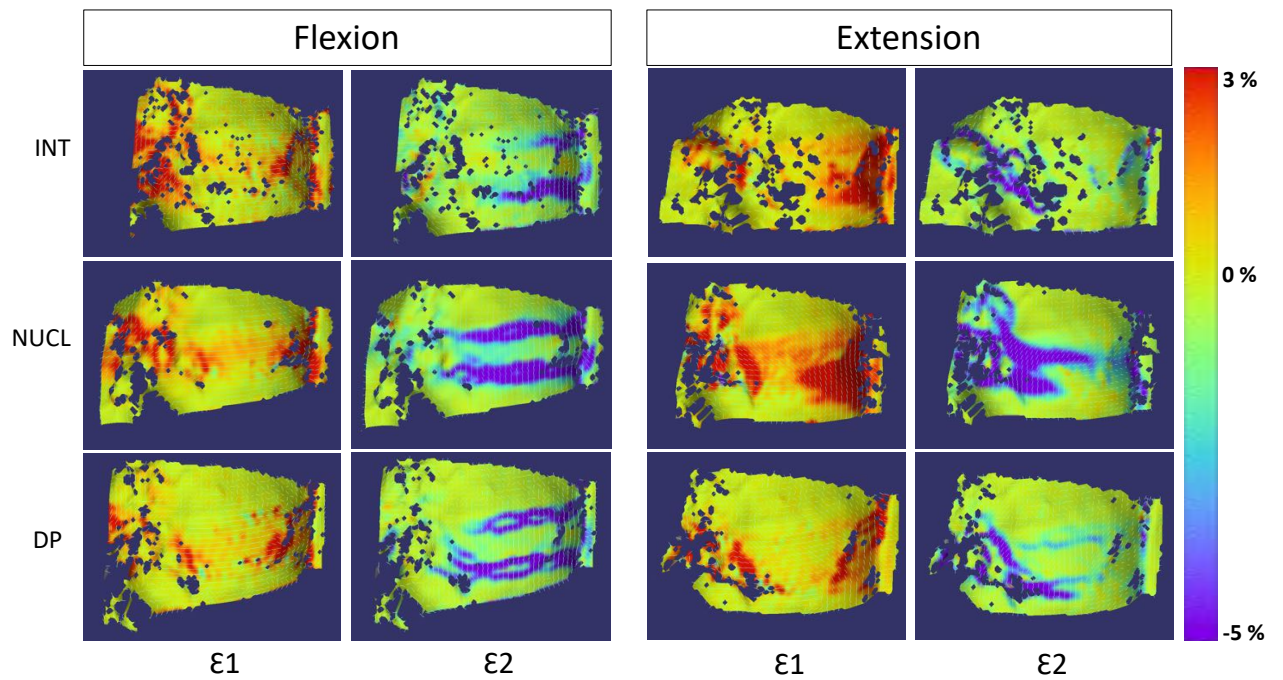
618 **Fig. 5** – Load-displacement curve of a representative specimen tested in extension in  
619 all disc conditions.

620



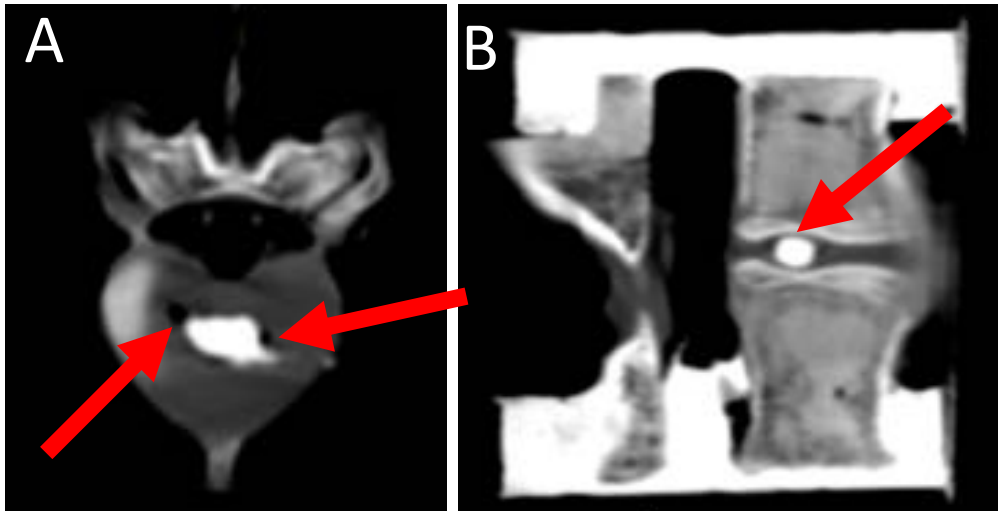
621

622 **Fig. 6** – Stiffness results in all conditions for all loading configurations. Average was  
623 done over all specimens. Normalized data were not statistically significant ( $p>0.1$ ).



625

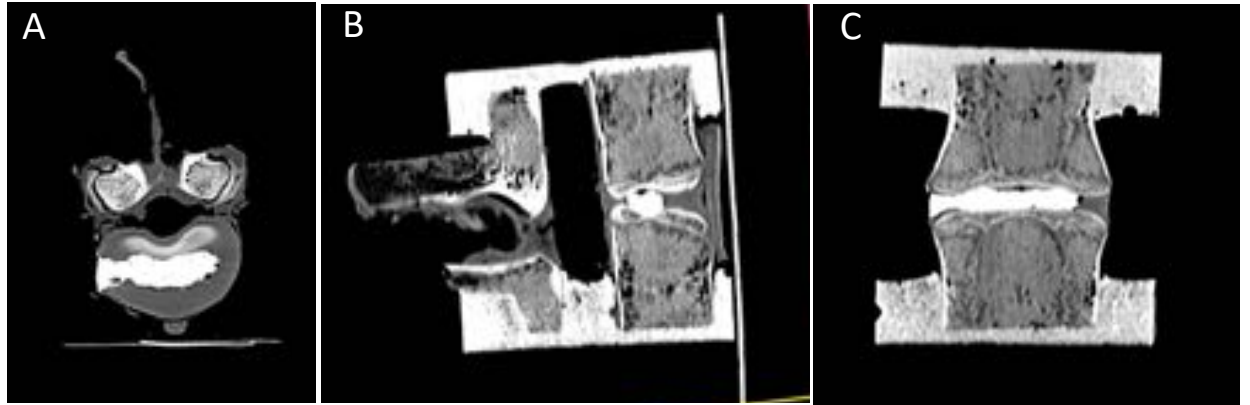
626 **Fig. 7** – Showed a typical strain distribution over a specimen surface for a flexion (left)  
 627 and extension (right) bending with first and second principal strains represented for  
 628 each motion.



629

630

631 **Fig. 8** –Sub optimal cement distribution. CT scans of porcine specimens in axial (A)  
632 and sagittal (B) planes. PMMA did not reach the annulus and the endplates (arrows),  
633 leaving vacuum.  
634



635

636 **Fig. 9** – Ideal distribution of the PMMA in the porcine model. CT scan of the porcine  
637 specimen, A (axial plane) the PMMA filled out the empty space after nucleotomy, B  
638 (sagittal plane) and C (coronal plane) the PMMA reached the two endplates and adapted  
639 to the geometry.

640 **TABLES**

641 *Table 1: Principal strains recorded over the disc surface in Flexion and Extension: The*  
 642 *mean and peak (of 10 specimens) are reported for  $\epsilon_1$  and for  $\epsilon_2$ .*

| $\epsilon_1$ | Flexion  |          | Extension |          |
|--------------|----------|----------|-----------|----------|
|              | Mean (%) | Peak (%) | Mean (%)  | Peak (%) |
| Intact       | 1.3±0.6  | 7.5±2.8  | 2.2±1.0   | 11.7±6.0 |
| Nucleotomy   | 1.3±0.7  | 10.5±7.1 | 1.9±0.6   | 10.1±3.9 |
| Discoplasty  | 1.0±0.5  | 8.7±3.5  | 1.2±0.7   | 10.0±4.1 |

643

| $\epsilon_2$ | Flexion  |           | Extension |            |
|--------------|----------|-----------|-----------|------------|
|              | Mean (%) | Peak (%)  | Mean (%)  | Peak (%)   |
| Intact       | -2.0±1.2 | -17.2±6.1 | -0.5±0.4  | -8.2±7.5   |
| Nucleotomy   | -2.8±1.6 | -18.7±8.9 | -1.7±1.5  | -12.5±10.4 |
| Discoplasty  | -1.7±0.9 | -16.5±7.3 | -0.7±0.8  | -13.3±5.3  |

644



645 *Table 2: Surface area and volume of the injected cement after segmentation.*

646

| <b>Specimen</b> | <b>Spine level</b> | <b>Cement surface<br/>area (mm<sup>2</sup>)</b> | <b>Cement volume<br/>(mm<sup>3</sup>)</b> |
|-----------------|--------------------|---|---|
| #1              | T13-L1*            | 257.8   | 282.8                                     |
| #2              | L3-L4              | 465.8   | 476.7                                     |
| #3              | T13-L1*            | 211.6   | 143.5                                     |
| #4              | L5-L6              | 623.7   | 673.9                                     |
| #5              | T13-L1*            | 712.3   | 750.3                                     |
| #6              | L3-L4              | 552.0   | 608.7                                     |
| #7              | L3-L4              | 742.2   | 776.5                                     |
| #8              | L3-L4              | 557.6   | 505.4                                     |
| #9              | T15-L1*            | 592.7   | 685.0                                     |
| Mean (SD)       | -                  | 524.0 (184.2)                                   | 544.8 (215.7)                             |

647 \* *Porcine spines have a variable number of thoracic vertebrae (between 13 and 15).*